DMD Fast Forward. Published on July 13, 2005 as doi:10.1124/dmd.104.003285

DMD #3285R2

TITLE PAGE

Metabolism of Pigment Yellow 74 by Rat and Human Microsomal Proteins

Yanyan Cui, Mona I. Churchwell, Letha H. Couch,
Daniel R. Doerge and Paul C. Howard

Division of Biochemical Toxicology (YC, MIC, LHC, DRD, PCH) and
National Toxicology Program Center for Phototoxicology (YC, LHC, PCH),
National Center for Toxicological Research,
U.S. Food and Drug Administration,
3900 NCTR Road,
Jefferson, AR USA 72079

RUNNING TITLE PAGE

Running Title: Microsomal Metabolism of Tattoo Pigment Yellow 74

Corresponding author:

Paul C. Howard, Ph.D.

Division of Biochemical Toxicology, HFT-110,

National Center for Toxicological Research,

U.S. Food and Drug Administration,

3900 NCTR Road, Jefferson, AR 72079

Telephone: (870)543-7672

Fax: (870)543-7136

E-mail: Phoward@nctr.fda.gov

Number of Text Pages: 32

Number of Tables: 1

Number of Figures: 7

Number of References: 42

Number of Words in Abstract: 202

Number of Words in Introduction: 598

Number of Words in Discussion: 1411

List of Nonstandard Abbreviations:

PY74, Pigment Yellow 74; PY74-M1 metabolite of PY74; PY74-M2 metabolite of PY74; MSDS, material safety data sheet; BSA, bovine serum albumin; 3-MC, 3-methylcholanthrene; DMSO, dimethylsulfoxide; PB, phenobarbital.

ABSTRACT

Pigment Yellow 74 (PY74) is a mono-azo pigment that is used in yellow tattoo inks. The metabolism of PY74 was investigated using rat liver and human liver microsomes and expressed human cytochromes P450 (CYP). Two phase I metabolites were isolated and characterized by MS and NMR techniques. One metabolite (PY74-M1) was a ring hydroxylation product of PY74, 2-((2-methoxy-4-nitrophenyl)azo)-*N*-(2-methoxy-4-hydroxyphenyl)-3-oxobutanamide. The second metabolite (PY74-M2) was identified as 2-((2-hydroxy-4-nitrophenyl)azo)-*N*-(2-methoxy-4-hydroxyphenyl)-3-oxobutanamide, which is the *O*-demethylation product of PY74-M1. These metabolites were formed by *in vitro* incubations of PY74 with 3-methylcholanthrene-induced rat liver microsomes and to a much lesser extent by liver microsomes from untreated or phenobarbital-induced rats. The role for cytochrome P450 (CYP) 1A in the metabolism of PY74 was confirmed using expressed human CYP's. The catalytic ability of the CYP's for metabolism of PY74 was CYP 1A2 > CYP 1A1 > CYP 3A4 ≈ CYP 1B1 (no activity with CYP 2B6, 2C9, 2D6 or 2E1). The metabolism of PY74-M1 to PY74-M2 was catalyzed only by CYP 1A2 and CYP 1A1 (no activity from CYP's 1B1, 2B6, 2C9, 2D6, 2E1 or 3A4). These results demonstrate the tattoo pigment PY74 is metabolized *in vitro* by CYP to metabolites that should be available for phase II metabolism and excretion**.**

INTRODUCTION

Pigment Yellow 74 (**Figure 1**) is a monoazo-based pigment that is manufactured under a variety of trade names and formulations for various industrial applications including coatings, offset inks, dry toner, liquid inks, and paint finishes. PY74 and other monoazo pigments are not manufactured for consumption or direct dermal application in humans, and are not listed as an approved color additive for use in foods, drugs, cosmetics or medical devices. PY74 is included in tattoo inks and permanent makeup that are available in Europe (Lehmann and Pierchalla, 1988; Danish Environmental Protection Agency, 2003; Bäumler et al., 2000, 2004; Papameletiou et al., 2003) and in the United States (Cui et al., 2004).

Tattooing is an ancient art form where colored materials are inserted into the skin with a sharp object. Recently, social/cultural trends in the US and other developed countries have resulted in a surge in the popularity of tattooing. Tattooing has been used recently as a permanent means to cover unwanted skin discoloration (*e.g.* vitiligo) or disfiguration (Mazza and Rager, 1993) or to correct skin color following some surgeries (Price et al., 2000); however, the single largest reason for voluntarily obtaining a tattoo has been personal artistic expression. In addition, permanent coloration of the lips and eyelids through tattooing is increasing in popularity and includes the application of black iron oxides and colored tattoo inks.

Tattooing has been identified as a significant risk factor for contraction of bacterial or viral (hepatitis and human immunodeficiency syndrome; HIV-AIDS)

infections (Long and Rickman, 1994; Haley and Fischer, 2001; Hayes and Harkness, 2001; Hellard et al., 2004). In addition to infectious diseases, other risks associated with tattooing (reviewed in Papameletiou et al., 2003) have included acute phototoxicity, granulomateous and lichenoid reactions, development of pseudo-lymphomas, immunological-based rejection of the tattoo, and unwanted pigment spreading or inconsistencies within the tattoo. There have been reports of non-melanoma skin cancer arising within tattoos (Weiner and Scher, 1987; McQuarrie, 1996; Jacob, 2002); however, these observations have not been substantiated by epidemiological studies.

The earliest tattoos were most likely derived from soot or charcoal with occasional inclusion of locally available minerals or plant products. In more recent times, inorganic compounds, such as titanium dioxide, mercuric oxide and cadmium sulfide, have been used in tattoo inks (Lehmann and Pierchalla, 1988). The demand for an increasing number of color shades and color intensity by customers and reports of toxicity of some of the inorganic salts has led tattoo ink manufacturers to replace the inorganic salts with organic pigments to achieve the desired colors and eliminate the toxicity associated with certain metal salts. Lehmann and Pierchalla (1988) and Bäumler et al. (2000) have listed many of these pigments, which include yellow, orange, blue, green, and red pigments commonly used in the paint and commercial printing industries. Little or no toxicity data have been reported for many of these pigments, even though they contain structural alerts for mutagenicity and/or carcinogenicity.

PY 74 is not listed as a hazardous substance with an LD_{50} for PY74 reported to be greater than 2,000 - 5,000 mg/kg in acute oral toxicity studies in rats, according to several Material Safety Data Sheets (MSDS); however, one MSDS does indicate an irritation or allergenicity hazard exists. There have been no reports to date regarding the *in vitro* or *in vivo* metabolism or *in vivo* disposition of PY74. The primary objective of our study was to investigate the *in vitro* metabolism of PY 74 by microsomal proteins and to identify the major metabolites for further evaluation of the safety of PY74 as part of our research program on tattoo ink safety.

METHODS

Chemicals and Materials

PY74 [2-((2-methoxy-4-nitrophenyl)azo)-*N*-(2-methoxyphenyl)-3-oxobutanamide; PY 74; CAS 6358-31-2; Color Index 11741], 3-nitroanisole, glucose-6-phosphate, glucose-6-phosphate dehydrogenase (Type XXIV), NADP (sodium salt), NADH, bovine serum albumin (BSA), 3-methylcholanthrene (3MC), dimethylsulfoxide (DMSO), anhydrous Na_2SO_4, and $MgCl_2$ were purchased from Aldrich/Sigma Chemical Co. (St. Louis, MO). Methanol and acetonitrile were HPLC grade and obtained from J. T. Baker (Phillipsburg, NJ, USA). Water was obtained by ion-exchange to >18 MOhm and filtered at 0.1 micron (Modulab 2020 UF, US Filter Corp., Lowell, MA, USA). All other reagents used were obtained in the highest purity from commercial sources.

Liver microsomes from male F344 rats pretreated with 3MC (intraperitoneal administration in corn oil for 3 consecutive days, 25 mg/kg body weight/day) were prepared by a standard procedure in our lab (Howard et al., 1988). The microsomal pellets were suspended in 250 mM sucrose, 50 mM potassium phosphate, pH 7.4, at approximately 20 mg/mL and stored at -80 ^{o}C . Protein content was determined using the method of Lowry et al. (1951). The total cytochrome P450 (CYP) content was calculated using the extinction coefficient 9.1×10^4 M^{-1} cm^{-1} from the difference spectrum of sodium dithionite-reduced and CO-saturated P450 according to the method of Johannesen and DePierre (1978). Human liver microsomes or male Sprague-Dawley rat liver microsomes from either untreated or phenobarbital (PB) pretreated rats were

purchased from In Vitro Technologies, Inc. (Baltimore, MD, USA). Human CYP supersomes containing expressed CYP's 1A1, 1A2, 1B1, 2B6, 2C9, 2D6, 2E1 and 3A4 (with cytochrome b_5) were purchased from BD Gentest (BD Biosciences Discovery Labware, Bedford, MA). The CYP concentration (1 nmol/mL) and protein concentrations of the expressed cytochromes were based on data supplied by manufacturer and were as follows (pmol CYP/mg protein): CYP 1A1, 45 pmol/mg; CYP 1A2, 71 pmol/mg; CYP 1B1, 91 pmol/mg; CYP 2B6, 160 pmol/mg; CYP 2C9, 179 pmol/mg; CYP 2D6, 106 pmol/mg; CYP 2E1, 91 pmol/mg; CYP 3A4, 106 pmol/mg.

Microsomal Incubations

The PY74 stock solution was prepared immediately before the assay by mixing 0.4 mL of 1.3 mM PY74 in DMSO with 10 mL water containing 10 mg/mL bovine serum albumin. The co-enzyme stock solution contained 2 mM NADP, 1.5 mM NADH, 20 mM glucose-6-phosphate, 2 units/mL glucose-6-phosphate dehydrogenase, 10 mM $MgCl_2$, and 100 mM potassium phosphate, pH 7.4. Immediately prior to use, 1 mg/mL microsomal protein was added. Equal amounts (250 μL) of the two solutions were mixed at 37 ^oC to start the reaction. Heat-inactivated microsomes (80 ^oC for 5 min) were used in control samples. In studies investigating the dependence of PY74 metabolism on protein, PY74, or BSA concentration, the incubations were stopped at 20 min. In the time course studies, the incubations were stopped at 10, 20, 30, 45, 60, 90 and 120 min. The incubation was stopped by the addition of 3 mL of methanol:CH_2Cl_2 (1:2) with

vigorous mixing. The CH_2Cl_2 was separated from the aqueous phase by centrifugation, the CH_2Cl_2 collected, and the water phase was further extracted with 2 mL of CH_2Cl_2. Following centrifugation, the organic phases were combined and 50 µL of internal standard (0.65 mM 3-nitroanisole in CH_2Cl_2) was added. The extract was dried using anhydrous Na_2SO_4 and evaporated *in vacuo* (SC210A Speed Vac Plus; Savant, Holbrook, NY, USA). The residue was reconstituted in 200 µL CH_2Cl_2 for HPLC analysis.

In the experiments to determine the specificity of human P450 isozymes in the metabolism of PY74, the incubations contained final concentrations of 0.25 nmol P450/mL, 1 mM NADP, 800 µM NADH, 10 mM glucose-6-phosphate, 1 unit/mL glucose-6-phosphate dehydrogenase, 4 mM $MgCl_2$, 10 mg/mL BSA, 50 mM potassium phosphate, pH 7.4, and 25 µM PY74 (or the metabolite PY74-M1). The total volume was 200 µL and incubation time was one hour at 37 ^oC. The extraction and HPLC analysis were the same as described above for microsomal metabolism of PY74.

High Performance Liquid Chromatography (HPLC)

HPLC analyses were carried out using a Waters liquid chromatography system (Waters Corp., Milford, MA) consisting of an Alliance 2695 separation Module and 2996 Photodiode Array (PDA) detector. The analyses were performed at ambient temperature (23 ^oC) on a Luna C_{18} column (4.6 x 150 mm, 3 µm particle size) protected by a Luna C_{18} guard column (3 x 4 mm) (Phenomenex, Torrance, CA, USA). The mobile phase flow rate was 800 µL/min

and consisted initially of 70:15:15 water:methanol:acetonitrile changing linearly to 5:47.5:47.5 over 50 minutes, and holding for 5 additional minutes. UV absorbance was monitored at 254 nm and injection volumes were 20 µL (see **Figure 2**).

Liquid Chromatography-Mass Spectrometry

The HPLC separation coupled with mass spectrometry was performed with a column and mobile phase that differed from the conditions used in the analytical studies. The solid phase was a Luna C_{18} column (2.1 x 150 mm, 3 micron particle, Phenomenex). The mobile phase had a flow rate of 200 µL/min delivered by a Waters Alliance 2795 system (Waters Corp.) and consisted of 70:15:15 water:methanol:acetonitrile changing linearly over 60 min to 10:45:45. An AD20 UV detector (Dionex, Sunnyvale, CA) was installed between the column and mass spectrometer and the UV absorption of the column eluate was monitored at 254 nm. For direct infusion studies, the sample was delivered at approximately 10 µL/ min using a syringe pump (KDS-100, KD Scientific Co., Boston, MA) into a tee with 200 µL/min of the initial gradient mobile phase as make-up flow before entering the mass spectrometer.

Mass spectra (MS/MS) were acquired on a Quattro Ultima triple quadrupole mass spectrometer (Waters Corp., Manchester, U.K.) equipped with an atmospheric pressure chemical ionization (APCI) interface (heated nebulizer probe at 400°C) and an ion source temperature of 120°C. Negative ion product spectra were acquired using a collision gas cell pressure (argon) of 1.8×10^{-3}

mbar and various collision energies, with a cone voltage of 40V. The corona pin was set at 20 µA and nitrogen was used as the cone gas and desolvation gas at 101 L/hr respectively.

Metabolite Isolation for NMR

All metabolites for NMR characterization were isolated from a 200 mL incubation using 500 µg/mL 3MC-induced rat liver microsomal protein, 1 mM NADP, 800 µM NADH, 10 mM glucose-6-phosphate, 1 unit/mL glucose-6-phosphate dehydrogenase, 4 mM $MgCl_2$, 25 µM PY74, and 10 mg/mL bovine serum albumin in 50 mM potassium phosphate, pH 7.4. After 1 hour, the solution was extracted with 400 mL of CH_2Cl_2:MeOH (2:1), then 2 times with 200 mL CH_2Cl_2. The organic phases were combined, dehydrated using anhydrous Na_2SO_4, then concentrated to 5-10 mL using evaporation under reduced pressure (Rotavapor-011, Büchi Labortechnik AG, Flawil, Swizerland). The products in the extract were separated using a 4.5 x 10 cm column of 60 Å (230-400 mesh) silica gel (Merck, Sigma-Aldrich). PY74 and a metabolite (PY74-M1) were eluted separately using CH_2Cl_2. A second metabolite (PY74-M2) was eluted from the column using a mobile phase of CH_2Cl_2:methanol (98:2).

The metabolite PY74-M1 was further purified using HPLC consisting of a Varian 9012 solvent delivery system (Varian, Walnut Creek, CA, USA) and a Luna C_{18} column (4.6 x 150 mm, 3 µm particle; Phenomenex). The isocratic mobile phase consisted of water:methanol:acetonitrile (30:35:35) with a flow rate of 1.0 mL/min. UV absorbance of the eluate was monitored at 254 nm using a

Varian 9050 Variable Wavelength UV-VIS detector. The fractions containing PY74-M1 were collected and dried *in vacuo*.

PY74-M2 was purified using 60Å silica gel column (30 x 65 mm) with CH_2Cl_2:methanol (99:1) as the eluant. The PY74-M2 fractions were collected and dried *in vacuo*.

NMR Spectroscopy

Proton NMR spectra were obtained at 500 MHz on a Bruker AM-500 spectrometer (Billerica, MA, USA). Compounds were dissolved in CD_2Cl_2 and all experiments were conducted at 28 ^{o}C. Chemical shifts are reported in ppm by assignment of the residual methylene chloride-d_1 peak ($CDHCl_2$) to 5.32 ppm. All NMR results are from first-order measurements using either DISNMR (Bruker) or 1D WIN-NMR (Bruker).

RESULTS

Microsomal Metabolism of PY74

PY74 was incubated with rat liver microsomal protein from 3MC-induced male F344 rat liver to determine if PY74 could be metabolized. As shown in **Figure 2**, two unidentified metabolites were separated by HPLC at 32.2 min (PY74-M2) and 35.1 min (PY74-M1) with UV-VIS spectra similar to the spectrum of PY74. The inclusion of heat-inactivated microsomal protein or the omission of the NADPH regenerating system did not result in the formation of these two

products (data not shown). A metabolite eluting at 35.8 min was the major product following incubation of PY74 with PB-induced male Sprague-Dawley rat liver microsomal protein; however, the total formation of metabolites from untreated and PB-induced microsomes were approximately ten-times less than those from inclusion of 3-MC-induced microsomal protein. The internal standard 3-nitroanisole had a maximum absorbance at 330 nm, eluted at ~20 min under the same chromatographic conditions (**Figure 2**) and was used in quantitative experiments.

PY74 has poor solubility in water. The solubility of PY74 in the microsomal incubations was increased by the inclusion of BSA. The metabolism of PY74 by 3MC-induced microsomes plateaued between 5-10 mg/mL BSA (results not shown), and therefore we used 5 mg/mL BSA in subsequent studies.

The metabolic activity increased significantly when the concentration of microsomal protein was increased from 100 µg/mL to 500 µg/mL, plateauing at 500 µg/mL with no additional increase in metabolism at 1 mg/mL (data not shown). The dependence of PY74 metabolism on PY74 concentration indicated a linear dependence of metabolism on the concentration of PY74 plateauing at 50 µM. Our initial intent was to conduct zero-order studies to understand the kinetics of PY74 metabolism; however, no kinetic analyses were conducted because of the complexity of the analysis (*i.e.* dependent on combined K_d of PY74 from BSA directly into microsomal lipid, PY74 solubility in microsomal lipid, solubility of PY74 in aqueous solution, and K_m and V_{max} properties of the CYP).

The incubation conditions for the rat liver microsomal protein and expressed human CYPs differed in the concentration of glucose-6-phosphate (10 and 5 mM, respectively) and BSA (5 and 10 mg/mL, respectively). The BSA concentration was adjusted in the human CYP studies in consideration of the low amount of CYP protein that was included in the assays. Since the studies with rat liver microsomal protein indicated the metabolism plateaued between 5-10 mg/mL BSA, it was felt the higher BSA concentration would not affect the qualitative results of the CYP assays. Similarly, since there was a low extent of CYP metabolism of both PY74 and PY74-M1, the reduced glucose-6-phosphate level in the CYP studies should not have affected the results.

The time course for the *in vitro* metabolism of PY74 by 3MC-induced rat liver microsomal protein was investigated, and is shown in **Figure 3**. The loss of PY74 plateaued after 30 minutes with consumption of approximately 20% of the substrate. Since PY74-M1 and PY74-M2 had essentially the same UV-VIS spectra (**Figure 2**), and since we did not have a method for quantifying PY74-M1 and PY74-M2 (*e.g.* ^{3}H or ^{14}C labeled), we assumed that the molar extinction coefficients for PY74, PY74-M1, and PY74-M2 were equal. As a result, the HPLC eluate was monitored at 420 nm and the peak areas of all eluting compounds were quantified. The formation of PY74-M1 and PY74-M2 paralleled the loss of PY74, with a greater accumulation of PY74-M1 than PY74-M2.

Identification of Microsomal Metabolites

The two microsomal metabolites of PY74 (*i.e.* PY74-M1 and PY74-M2) were generated and purified as described in Materials and Methods. PY74-M1 was analyzed using HPLC coupled with negative ion APCI mass spectrometry. PY74-M1 showed parent ion [$(M-H)^-$] at *m/z* 401 (**Figure 4A**) which is consistent with PY74-M1 being a hydroxylation product of PY74 (386 Da for PY74 + 16 Da for O). The major fragment ions obtained from PY74-M1 were *m/z* 236 and *m/z* 167, consistent with cleavage of the R=N-NH-R bond as shown in **Figure 4A**, as has been previously shown for PY74 (Cui et al., 2004). Fractions of *m/z* 221 and 152 were either demethylation or deamination fragments from *m/z* 236 and 167, respectively. Taking into consideration the fragmentation of PY74 (Cui et al., 2004) the fragmentation of PY74-M1 is consistent with hydroxylation on the amino-anisole ring (C1"-C6") and not the on the amino-nitro-anisole ring (C1'-C6').

The NMR spectrum of PY74-M1 was obtained and compared to the previously assigned spectrum of PY74 (Cui et al., 2004). Examination of the spectrum (not shown) for PY74-M1 revealed that all proton resonances from PY74 are present with the exception of the H4" proton at 7.13 ppm (**Table 1**). The resonance for proton H3" in PY74-M1 is shifted upfield by 0.46 ppm as compared to H3" in PY74 suggesting hydroxyl substitution at an adjacent (*ortho*) carbon. H3" in PY74-M1 has only a long-range *meta*-coupling of 2.7 Hz to H5", whereas, H3" in PY74 has predominantly an *ortho* coupling of 8.1 Hz to H4", and *meta* coupling to H5". Similarly, the resonance for proton H5" in PY74-M1 is shifted upfield by 0.56 ppm when compared to H5" in PY74 suggesting hydroxyl

ortho-substitution. The chemical shift for H6" in PY74-M1 is 0.19 ppm upfield from H6" in PY74 indicating the 6-position is *meta* to the site of substitution on the ring. The resonances for H6" and H5" in PY74-M1show *ortho* coupling constants (8.7 Hz). Taking into account these observations, we conclude the site of hydroxylation on PY74-M1 is the C4" position as shown in **Figure 4A**. The appearance of a substantially broadened resonance at 4.94 ppm (**Table 1**) is attributable to the 4"-OH. The combined LC/MS and NMR analysis support that the structure of PY74-M1 is 2-((2-methoxy-4-nitrophenyl)azo)-*N*-(2-methoxy-4-hydroxyphenyl)-3-oxo-butanamide.

The addition of PY74-M1 to microsomal incubations containing 3MC-induced rat liver microsomes indicated that PY74-M1 is metabolized to PY74-M2 (data not shown). The APCI negative ion MS analysis of purified PY74-M2 is shown in **Figure 4B**, and indicates a parent ion [$(M-H)^-$] at *m/z* 387, which is a loss of 14 Da from PY74-M1. The most probable structure of PY74-M2 to account for this mass is a demethylation product of PY74-M1. Fragmentation ions at *m/z* 152 and *m/z* 222 (**Figure 4B**) suggest that the site of demethylation is the methoxy group on the amino-nitro-anisole ring (C1'-C6') and not the amino-anisole ring (C1"-C6").

The proton NMR spectrum of PY74-M2 confirmed the site of demethylation. PY74-M2 had the same number of proton resonances and a similar coupling pattern as that of PY74-M1, with the one notable exception that there was only a single methoxy resonance (integrated to approximately 3 hydrogens) at 3.93 ppm indicating a loss of one of the methoxy groups (**Table 1**).

The chemical shift of this methoxy group (3.93 ppm) was the same as that of the C7" methoxy in PY74-M1 which was only shifted 0.04 ppm upfield from the C7" group in PY74 (**Table 1**). The resonance of the methoxy group at C7' [4.08 ppm in PY74-M1 and 4.09 ppm in PY74] was not present in PY74-M2. This suggested PY74-M2 was the C7' *O*-demethylation product of PY74-M1. This assignment is further supported by a 0.29 ppm upfield shift for the H6' proton which is *meta* to the C7' hydroxyl. Thus, the structure of PY74-M2 was identified as 2-((2-hydroxy-4-nitrophenyl)azo)-*N*-(2-methoxy-4-hydroxyphenyl)-3-oxo-butanamide. This metabolite is not stable in water at room temperature and decomposes to more polar compounds.

Metabolism of PY74 and PY74-M1 by Human Cytochromes P450

The incubation of PY74 with human liver microsomes (not shown) resulted in the formation of predominantly PY74-M1 and PY74-M2, with one minor peak that was less polar than PY74-M1 which was not identified due to lack of sufficient material. The specificity of the human CYP metabolism of PY74 is shown in **Figure 5**, where CYP 1A2 had the highest activity followed by CYPs 1A1, 3A4 and 1B1. CYP 2B6, 2C9, 2D6 and 2E1 did not metabolize PY74. CYP 1A1 and CYP 1A2 metabolized PY74 to both PY74-M1 and PY74-M2 at a ratio of approximately 5.6:1, while CYP1B1 formed exclusively PY74-M1 (data not shown).

CYP 1A1 and CYP1A2 metabolized PY74-M1 to only PY74-M2 (**Figure 6**). The other CYP's did not metabolize PY74-M1.

DISCUSSION

This is the first report describing the metabolism of PY74 by microsomal proteins or cytochromes P450 and the specificity of the site of metabolism (**Figure 7**). This work is of public health significance because many individuals are being tattooed with this pigment as color component of some yellow tattoo inks (Lehmann and Pierchalla, 1988; Bäumler et al., 2000; Cui et al., 2004). To date, neither the metabolism of PY74 nor the description of the identity of any metabolites of PY74 has been presented.

We find that PY74 is metabolized by microsomal protein from 3MC-induced rat livers. 3MC is an inducer of CYP1A proteins (Tanaka, et al., 1997). We found the PY74 metabolism by microsomal proteins from non-induced or phenobarbital-induced rat livers was considerably less than that from the 3MC-induced livers. This is consistent with our observations that CYP 1A1 and 1A2 were the isoforms responsible for PY74 metabolism because phenobarbital is an inducer primarily of CYP 2B's and to some extent 3A's (Martignoni et al., 2004). These data are consistent with the human CYP-specificity of PY74 metabolism where CYP1A1 and CYP1A2 had the highest activity of the tested CYP's for PY74 metabolism (**Figure 5**). We found that PY74-M1 is also preferentially metabolized by CYP1A1 and 1A2 to its *O*-demethylated product (**Figure 6**). These data suggest that tissue expressing CYP1A1 or CYP1A2 would have the capacity to metabolize PY74.

The skin is an important organ in the human body, not only serving as a barrier to the environment, but it also has the capacity to metabolize chemicals that enter the body by absorption through the skin. The skin does contain CYPs, albeit at low levels compared to other organs such as the liver and kidney (Mukhtar and Khan, 1989). The CYPs in skin can be induced several-fold by a wide variety of substrates (Mukhtar and Bickers, 1981; Mukhtar and Khan, 1989) and are altered by exposure to ultraviolet light (Goerz et al., 1996). Janmohamed et al. (2001) have reported that mRNAs for CYP 2A6, 2B6, and 3A4 are expressed in human skin taken from surgical samples, and that these CYP's were primarily located in the epidermis, sebaceous glands, and hair follicles. Yengi et al. (2003) reported the presence of mRNA for CYP 1A1, 1B1, 2B6, 2C9, 2C18, 2C19, 2D6, 2E1, 3A4 and 3A5 in human skin, while CYP 1A2, 2A6, and 2C8 mRNA levels were below the detection limits of their assay. Ahmad et al. (1996) reported CYP 1A1 was the major CYP in rodent skin, which is consistent with reports of the induction of CYP activity in the skin of rodents treated with 3MC and other inducers of CYP 1A. Du et al. (2004) reported 13 cytochromes of the CYP2 family, including 2A6, 2A7, 2B6, 2C9, 2C18, 2C19, 2D6, 2E1, 2J2, 2R1, 2S1, 2U1, and 2W1, were present in human skin samples. In summary, the skin contains many different CYPs, which have been detected as either mRNA, enzyme activities or protein levels.

Our work has shown that PY74 is metabolized by human CYP1A1, CYP1A2, 1B1, and 3A4. These CYPs are present in the skin of rodents and humans, suggesting that metabolism of PY74 could occur there *in vivo*.

We have identified the major metabolite of PY74 as the 4"-hydroxylation product PY74-M1 through both MS and NMR techniques. Our conclusion that PY74 is hydroxylated at the 4" position is consistent with the work of Sapota et al (2003) who demonstrated that administration of 2-methoxyaniline (*o*-anisidine) to rats results in the excretion of *N*-acetyl-2-methoxyaniline and *N*-acetyl-4-hydroxy-2-methoxyaniline. *O*-anisidine and its *N*-acetyl derivative are structurally very similar to the C1"-C6" ring system on PY74.

The second metabolite is an *O*-demethylation of PY74-M1 by CYP1A1 and 1A2. Many CYPs are capable of *O*-demethylation of xenobiotics. For example, CYP 2D6 catalyzes the *O*-demethylation of dextromethorphan, hydrocodone, 5-methoxy-N,N-dimethyltryptamine, and pinoline.

We believe our results demonstrate PY74-M1 is sequentially converted to PY74-M2. First, the incubation of PY74-M1 with either microsomal protein or CYP resulted in the formation of PY74-M2 (Figure 6). Second, the structures of PY74-M1 and PY74-M2 are consistent with sequential metabolism. Third, additional metabolites such as the 7'-*O*-demethylation of PY74 which would be expected as a precursor to PY74-M2 were not detected. If labeled (^{3}H, ^{13}C, or ^{14}C) PY74 becomes available, future experiments would be able to confirm the proposed sequential metabolism of PY74 to PY74-M1 and then PY74-M1 to PY74-M2.

PY74 is a nitro-aromatic compound that contains an azo (or hydrazone; Cui et al., 2004) group. Many azobenzenes have been reported to be reduced to primary amines by CYP's and NADPH-cytochrome P450 reductase (Levine,

1991). Metabolic azoreduction and cleavage is believed to be an activation reaction since the reduction products of some azo compounds exhibit toxic and mutagenic effects (Chung, 1983; Martin and Kennelly, 1985). A structure-activity study of various azobenzenes revealed that a polar electron-donating group (amino or hydroxyl) *para* to the azo linkage is required for substrate activity with microsomes. An electron-withdrawing group, such as a nitro group, on the benzoyl moiety prevents electron donation to the azo ring system and the resulting product is inactive in azo reduction (Zbaida, 1995). Although we did not examine the azoreduction of PY74 by skin microsomes or cytosol in our metabolic system, skin azoreduction of several azo compounds including ANSC [5-(phenylazo)-6-hydroxynaphthalene-2-sulfonic acid], Sudan I (1-phenylazo-2-naphthol; C.I. 12055), and Solvent Yellow 7 (4-phenylazophenol; C.I. 11800) have been demonstrated with a percutaneous absorption system (Collier et al., 1993). Therefore, the potential for azoreduction of PY74 by skin does exist and should be investigated. In addition, simulated solar light (Cui et al., 2004) and laser light used for tattoo removal (Vasold et al., 2004) have been shown to photochemically cleave PY74 at the azo group to generate aromatic amines, such as 2-methoxy-4-nitroaniline and 2-aminoanisole from PY74.

Under the definitions given in the Food Drug and Cosmetic Act, and associated regulations in 21 US Code of Federal Regulations Title 21, tattoo inks have been categorized by the FDA to be professional use cosmetics. As a result, the pigments contained in the inks are considered to be color additives. Both cosmetics and color additives fall under the regulatory authority of FDA.

Although individuals are encouraged to report adverse events resulting from FDA-regulated products to the US Food & Drug Administration, the lack of public perception that tattoo inks are regulated by the FDA probably explains why few complaints have been received, explaining why a comprehensive assessment or database on adverse events resulting from tattooing does not exist.

The results described in this paper show that tattoo ink pigments can be metabolized by phase I enzymes (CYPs) that exist in the skin of rodents and man. Anecdotal reports of tattoo fading are routinely heard from tattoo recipients who have yellow and orange tattoos. We suggest the mechanisms for fading could include: (1) dispersion through the skin; (2) phagocytosis and removal; (3) metabolism of the pigments in the skin (this report); (4) photochemical decomposition of the pigments as reported for PY74 (Cui et al., 2004; Vasold et al., 2004). No reports exist regarding the mutagenic, carcinogenic, or photocarcinogenic potential of PY74; however, 2-aminoanisole (*o*-anisidine) can be enzymatically activated *in vitro* to form DNA adducts (Stiborova et al., 2001, 2002) and is a urinary bladder carcinogen in mice and rats (National Toxicology Program, 1978). Oxidation of PY74-M1 could result in the formation of structure similar to a p-quinone imine, which is the active intermediate for o-anisidine (Stiborova et al., 2002) and acetaminophen (NAPQI; Rogers et al., 1997). In order to conduct a risk assessment for PY74, further studies on the purity of PY74 used in tattoo inks, the *in vivo* metabolism of PY74 in the skin, and quantification of the toxicity of its metabolites are among some of the studies that are warranted.

ACKNOWLEDGEMENTS

The authors would like to thank F.E. Evans and F.A. Beland for the NMR analyses.

REFERENCES

Ahmad N, Agarwal R and Mukhtar H (1996) Cytochrome P-450 dependent drug metabolism in skin. *Clinics Dermatology* **14**: 407-415.

Bäumler W, Eibler ET, Hohenleutner U, Sens B, Sauer J, and Landthaler M. (2000) Q-switched laser and tattoo pigment: first results of the chemical and photophysical analysis of 41 compounds. *Lasers Surg. Med*. **26**: 13-21.

Brede C, Skjevrak I, Fjeldal P. (2003) Colour substances in food packaging materials., Working report for the Norwegian Food Control Authority, 3/03, ISSN 1503 – 2345. http://www.snt.no/dokumentasjon/rapporter/2003/snt_arbeidsrapporter/200303.pdf.

Chung KT (1983) The significance of azo-reduction in the mutagenesis and carcinogenesis of azo dyes. *Mutat Res* **114**: 269-281.

Collier SW, Storm JE, and Bronaugh RL. (1993) Reduction of azo dyes during *in vitro* percutaneous absorption. *Tox. Appl. Pharmacol*. **118**: 73-79.

Cui Y, Spann AP, Couch LH, Gopee NV, Evans FE, Churchwell MI, Williams LD, Doerge DR, and Howard PC (2004) Photodecomposition of Pigment Yellow 74, a pigment used in tattoo inks. *Photochemistry and Photobiology* **80**:175-184.

Danish Environmental Protection Agency (2003) Chemicals in consumer products. Available at http://www.mst.dk/chemi/01080200.htm (last accessed 5 October 2004)

DeVito MJ, Menache MG, Diliberto JJ, Ross DG, and Birnbaum LS (2000) Dose-response relationships for induction of CYP1A1 and CYP1A2 enzyme activity in liver, lung, and skin in female mice following subchronic exposure to polychlorinated biphenyls. *Toxicol Applied Pharmacol* **167**: 157-172.

Du L, Hoffman SMG, and Keeney DS. (2004) Epidermal CYP2 family cytochromes P450. *Tox. Appl. Pharmacol*. **195**: 278-287.

FDA. (1998) Latex condoms for men information for 501(k) premarket notifications: Use of consensus standards for abbreviated submissions. (available at: http://www.fda.gov/cdrh/ode/92_b.html; last accessed 24 August 2004).

Goerz G, Barnstorf W, Winnekendonk G, Bolsen K, Fritsche C, Kalka K, and Tsambaos D (1996) Influence of UVA and UVB irradiation on hepatic and cutaneous P450 isoenzymes. *Arch Dermatol Res.,* **289**: 46-51.

Haley RW and Fischer RP (2001) Commercial tattooing as a potentially important source of hepatitis C infection. Clinical epidemiology of 626 consecutive patients unaware of their hepatitis C serologic status. *Medicine* **80**: 134-151.

Hayes MO and Harkness GA (2001) Body piercing as a risk factor for viral hepatitis: an integrative research review. *Am J Infect Control* **29**: 271-274.

Hellard ME, Hocking JS, and Crofts, N. (2004) The prevalence and the risk behaviours associated with the transmission of hepatitis C virus in Australian correctional facilities. *Epidemiol. Infection* **132**: 409-415.

Howard PC, Mateescu D and Consolo MC (1988) Liver microsomal metabolism of the environmental carcinogen 3-nitrofluoranthene. I. Phenolic metabolites. *Carcinogenesis* **9**: 911-917.

Jacob CI (2002) Tattoo-associated dermatoses: A case report and review of the literature. *Dermatol Surg* **28**: 962-965.

Janmohamed A, Dolphin CT, Phillips IR, and Shephard EA (2001) Quantification and cellular localization of expression in human skin of genes encoding flavin-monooxygenases and cytochromes P450. *Biochem Pharmacol*. **62**: 777-786.

Johannesen KA and DePierre JW. (1978) Measurement of cytochrome P-450 in the presence of large amounts of contaminating hemoglobin and methemoglobin. *Analy Biochem* **86**:725-732.

Lehmann G von, and Pierchalla P. (1988) Tätowierungsfarbstoffe. *Derm. Beruf. Umwelt*. **36**: 152-156.

Levine WG (1991) Metabolism of azo dyes: implication for detoxication and activation. *Drug Metab Rev* **23**: 253-309.

Long GE, and Rickman LS. (1994) Infectious complications of tattoos. *Clinical Infectious Diseases* **18**: 610-619.

Lowry OH, Rosebrough NJ, Farr AL, and Randall R. (1951) Protein measurement with the Folin phenol reagent. *J. Biol. Chem.* 193: 265-275.

Martin CN and Kennelly JC (1985) Metabolism, mutagenicity, and DNA binding of biphenyl-based azo dyes. *Drug Metab Rev* **16**: 89-117.

Mazza JF Jr and Rager C (1993) Advances in cosmetic micropigmentation. *Plastic & Reconstructive Surgery* **92**: 750-751.

McQuarrie DG (1996) Squamous-cell carcinoma arising in a tattoo. *Minn Med* **49**: 799-801.

Martignoni M., de Kanter R., Grossi P., Mahnke A., Saturno G., and Monshouwer M. (2004) An in vivo and in vitro comparison of CYP induction in rat liver and intestine using slices and quantitative RT-PCR. *Chemico.-Biol. Interact*. **151**: 1-11.

Mukhtar H, and Bickers DR (1981) Comparative activity of the mixed-function oxidases, epoxide hydrolase, and glutathione S-transferase in liver and skin of the neonatal rat. *Drug Metabol DIspos*. **9**: 311-314.

Mukhtar H and Khan WA (1989) Cutaneous cytochrome P-450. *Drug Metabolism Reviews* **20**: 657-673.

Mutalik S and Ginzburg A (2000) Surgical management of stable vitiligo: A review with personal experience. *Dermatological Surgery* **26**: 248-254.

National Toxicology Program (1978) Bioassay of *o*-anisidine hydrochloride for possible carcinogenicity. NTP Technical Report 78. (available at http://www.ntp-server.niehs.nih.gov; accessed 24 August 2004)

Papameletiou D, Zenié A., Schwela D, and Bäumler W. (2003) Risks and health effects from tattoos, body piercing, and related practices. Report to European Commission Directorate General. Available at http://europa.eu.int/comm/consumers/cons_safe/news/eis_tattoo_risk_052003_en.pdf (last accessed 5 October 2004)

Price N, Gottfried MR, Clary E, Lawson DC, Billie J, Mergener K, Westcott C, Eubanks S and Pappas TN (2000) Safety and efficacy of India ink and indocyanine green as colonic tattooing agents. *Gastrointestinal Endoscopy* **51**: 438-442.

Rogers LK, Moorthy B, and Smith CV. (1997) Acetaminophen binds to mouse hepatic and renal DNA at human therapeutic doses. *Chem. Res. Toxicol*. **10**:470-476.

Sapota A, Czerski B, and Jędrzejczak M. (2003) Tissue distribution , excretion and metabolism of o-anisidine in rats. *Int. J. Occup. Medicine Environ. Health* **16**: 351-357.

Silvers KJ, Chazinski T, McManus ME, Bauer SL, Gonzalez FJ, Gelboin HV and Maurel P and Howard PC. Cytochrome P450 3A4 is responsible for the C-oxidative metabolism of 1-nitropyrene in human liver microsomal samples. *Cancer Research* **52**: 6237-6243.

Stiborova M, Schmeiser HH, Bruer A, and Frei E. (2001) Evidence for activation of carcinogenic o-anisidine by prostaglandin synthase: ^{32}P-postlabeling analysis of DNA adduct formation. *Gen. Physiol. Biophys*. **20**: 267-279.

Stiborova M, Miksanova M, Havlicek V, Schmeiser HH, and Frei E. (2002) Mechanism of peroxidase-mediated oxidation of carcinogenic o-anisidine and its binding to DNA. *Mutation Res*., **500**: 49-66.

Tanaka T, Watanabe J, Asaka Y, Ogawa R and Kanamura S (1997) Quantitative analysis of endoplasmic reticulum and cytochrome P-450 in hepatocytes from rats injected with methylcholanthrene. *Eur J Cell Biol* **74**: 20-30.

Vasold R, Naarmann N, Ulrich H, Fischer D, König B, Landthaler M, and Bäumler W. (2004) Tattoo pigments are cleaved by laser light – the chemical analysis in vitro provide evidence for hazardous compounds. *Photochem. Photobiol*. **80**:185-190.

Weiner DA and Scher RK (1987) Basal cell carcinoma arising in a tattoo. *Cutis* **39**: 125-126.

Yengi LG, Xiang Q, Pan J, Scatina J, Kao J, Ball SE, Fruncillo R, Ferron G, and Wolf RG (2003) Quantitation of cytochrome P450 mRNA levels in human skin. *Analy. Biochem*. **316**: 103-110.

Zbaida S. (1995) the mechanism of microsomal azoreduction: predictions based on electronic aspects of structure-activity relationships. *Drug Met. Rev.* **27**: 497-516.

FOOTNOTES

The contents of this manuscript do not necessarily reflect the views or policies of the US Food & Drug Administration, nor does the mention of trade names or commercial products constitute endorsement or recommendation for use. Y. Cui was supported by an appointment to the Oak Ridge Affiliated Universities Research Program at the National Center for Toxicological Research, administered through an interagency agreement between the US Department of Energy and the US Food & Drug Administration. The funding support from the Office of Food Additive Safety, Center for Food Safety and Applied Nutrition (CFSAN), US Food & Drug Administration is acknowledged. The NTP Center for Phototoxicology is supported in part by an Interagency Agreement (IAG 224-93-0001) between the US Food & Drug Administration and the US National Institute for Environmental Health Sciences.

LEGENDS FOR FIGURES

Figure 1. Structure of Pigment Yellow 74 (PY74).

Figure 2. HPLC separation of PY74 and its metabolites (PY74-M1 and PY74-M2) following incubation with 3MC-induced rat liver microsomes. The column eluant was monitored for UV absorbance at 254 nm. The inset shows the UV-VIS spectrum of PY74 and the two metabolites. The peak outlined by the dashed line at approximately 19.6 min is due to the absorbance of the internal standard.

Figure 3. The time course of PY74 metabolism. The total peak areas of PY74, PY74-M1 and PY74-M2 at 420 nm were normalized to 100% (n=3). The left axis depicts the decrease in PY74 (solid line) at the indicated time-points. The right axis depicts the peak area ratios for PY74-M1 and PY74-M2.

Figure 4. The negative ion LC/MS of PY74-M1 (panel A) and PY74-M2 (panel B).

Figure 5. Metabolism of PY74 by expressed human cytochromes P450. The results are from triplicate determinations.

Figure 6. Metabolism of PY74-M1 by expressed human cytochromes P450. The results are from triplicate determinations.

Figure 7. Scheme for metabolism of PY74 by cytochromes P450.

DMD Fast Forward. Published on July 13, 2005 as DOI: 10.1124/dmd.104.003285
This article has not been copyedited and formatted. The final version may differ from this version.

TABLES

Table 1. ^{1}H-NMR spectral parameters for PY74, PY74-M1 and PY74-M2 [a]

Position	PY74 (δ, ppm)	PY74-M1 (δ, ppm)	PY74-M2 (δ, ppm)
1-NH	11.65 (bs, 1H)	11.48 (bs, 1H)	11.48 (bs, 1H)
2-NNH	14.74 (bs, 1H)	14.76 (bs, 1H)	15.09 (bs, 1H)
4	2.61 (s, 3H)	2.60 (s, 3H)	2.56 (s, 3H)
H3'	7.86 (d, 1H)	7.85 (d, 1H)	7.82 (d, 1H)
H5'	7.98 (dd, 1H)	7.97 (dd, 1H)	7.88 (dd, 1H)
H6'	7.78 (d, 1H)	7.77 (d, 1H)	7.48 (d, 1H)
7'	4.09 (s, 3H)	4.08 (s, 3H)	-
H3"	6.98 (dd, 1H)	6.52 (d, 1H)	6.51 (d, 1H)
H4"	7.13 (dt, 1H)	-	-
H5"	6.99 (dt, 1H)	6.43 (dd, 1H)	6.43 (dd, 1H)
H6"	8.41 (dd, 1H)	8.22 (d, 1H)	8.19 (d, 1H)
7"	3.97 (s, 3H)	3.93 (s, 3H)	3.93 (s, 3H)
4"-OH	-	4.94 [b]	-
	$J_{3',5'}$ = 2.3 Hz $J_{5',6'}$ = 8.9 Hz $J_{3",4"}$ = 8.1 Hz $J_{3",5"}$ = 1.4 Hz $J_{4",5"}$ = 7.5 Hz $J_{4",6"}$ = 1.4 Hz $J_{5",6"}$ = 8.1 Hz	$J_{3',5'}$ = 2.3 Hz $J_{5',6'}$ = 8.9 Hz $J_{3",5"}$ = 2.7 Hz $J_{5",6"}$ = 8.7 Hz	$J_{3',5'}$ = 2.4 Hz $J_{5',6'}$ = 9.0 Hz $J_{3",5"}$ = 2.5 Hz $J_{5",6"}$ = 8.6 Hz

[a]: Recorded in CD_2Cl_2 at 500 MHz, Chemical shift (δ) values in ppm and coupling constant (*J*) values in Hz. Splitting patterns: s, singlet; bs, broad singlet; d, doublet; dd, double of doublets; dt, double of triplets.

[b]: Substantially broadened resonance, assigned as –OH.

FIGURE 1

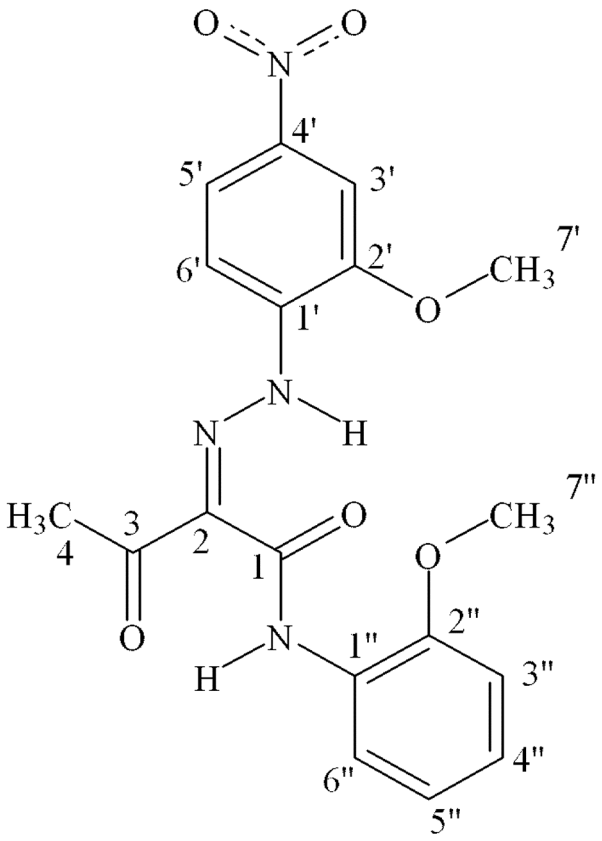

FIGURE 2

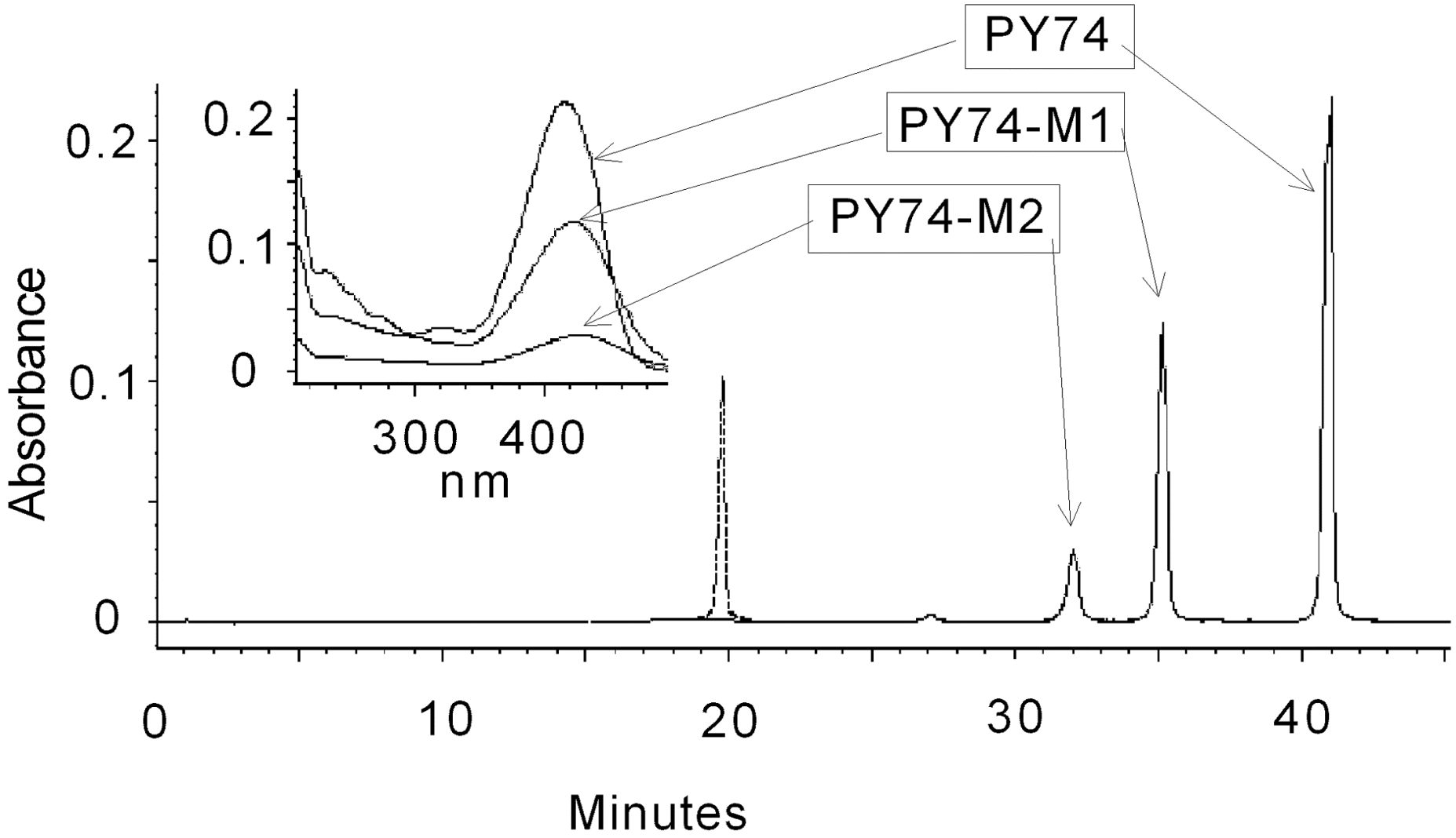

FIGURE 3

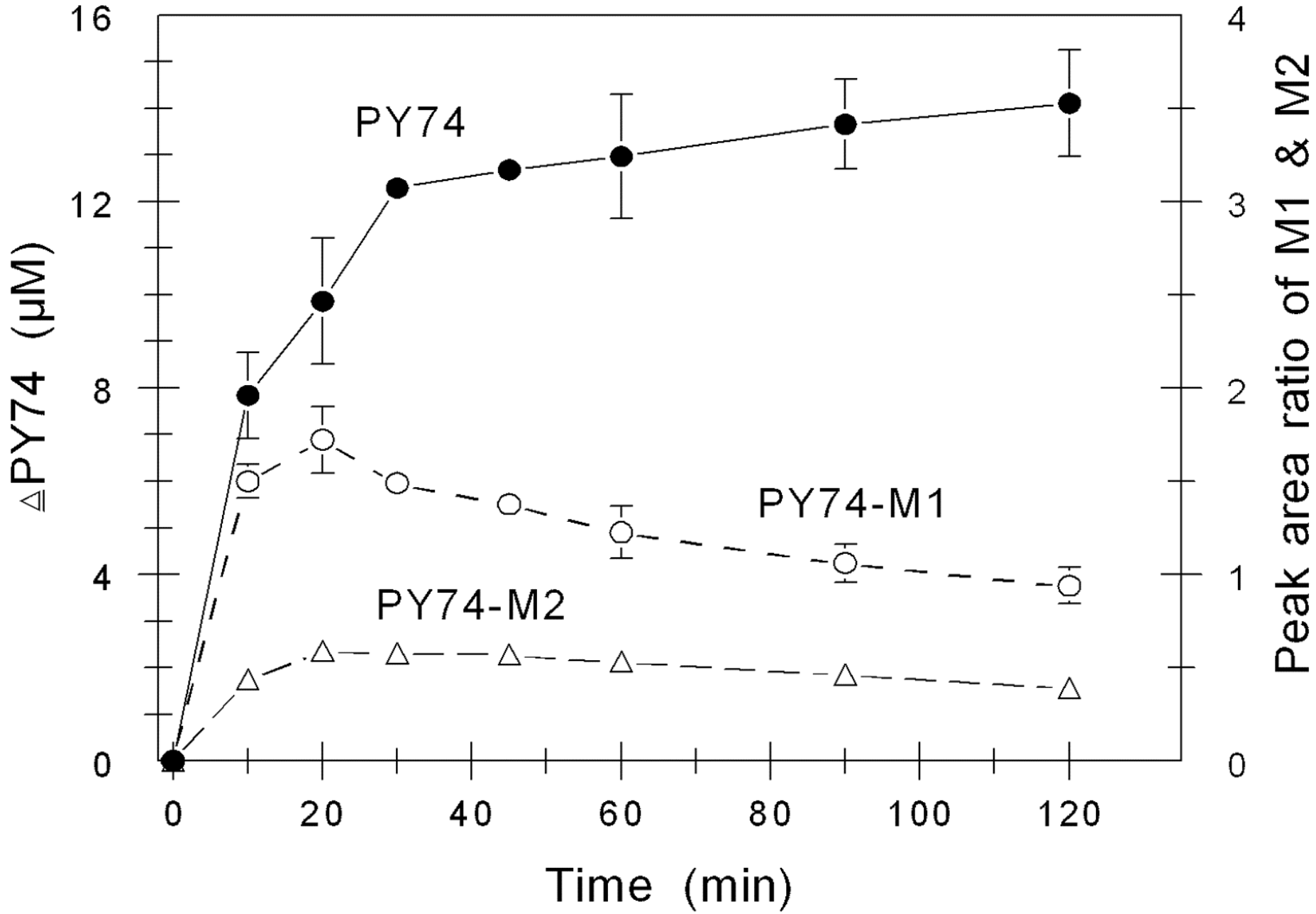

FIGURE 4

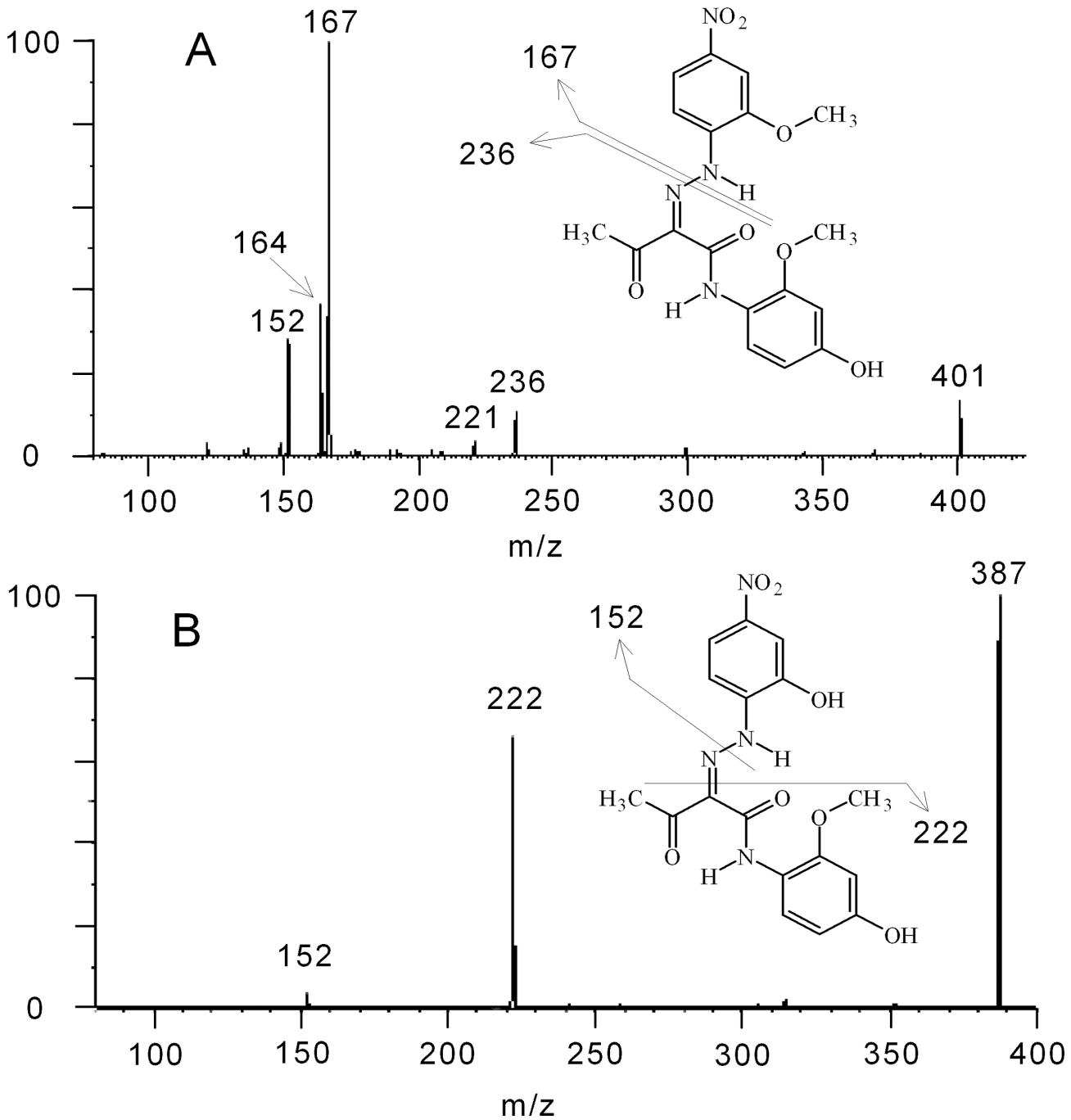

FIGURE 5

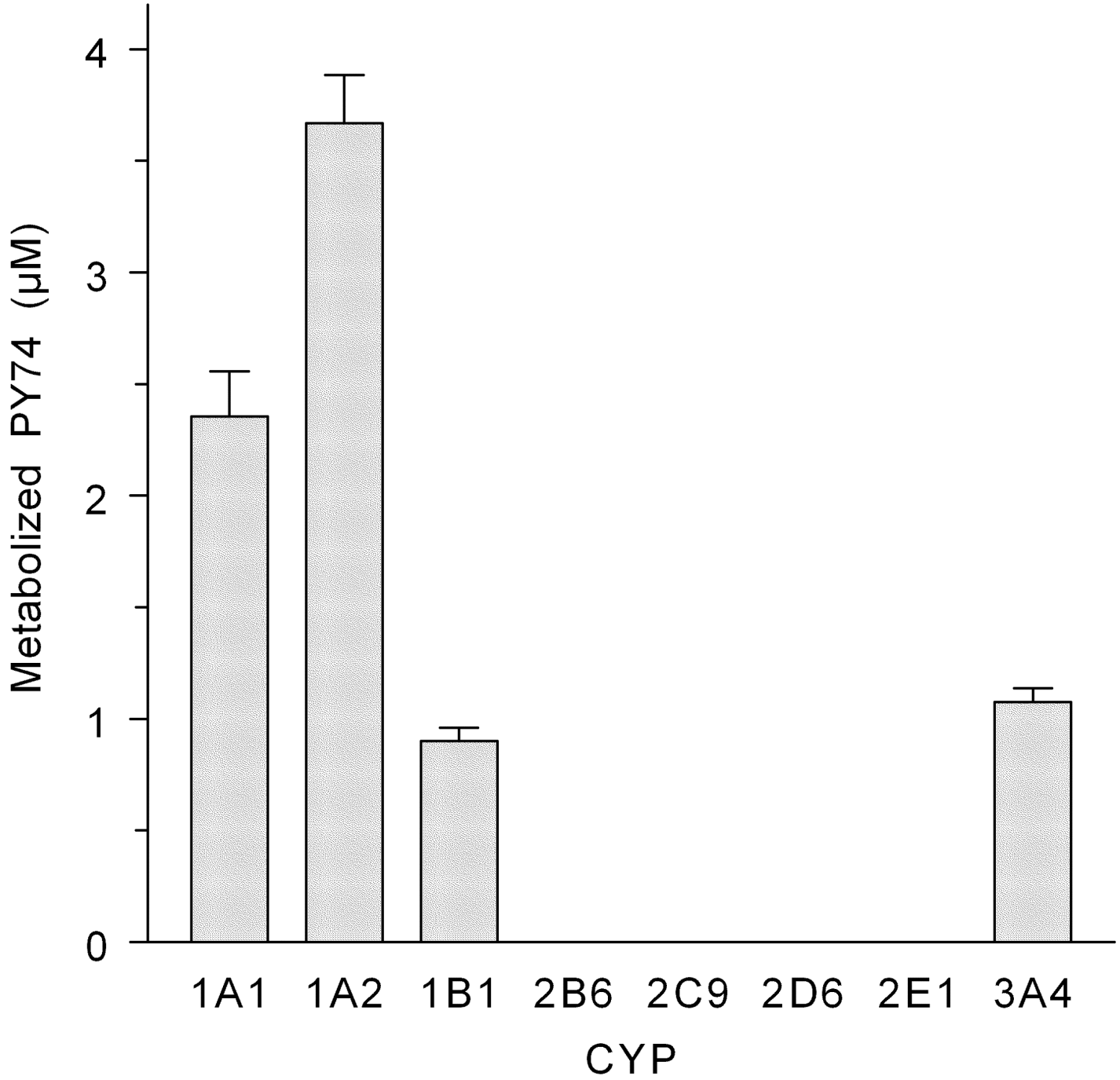

FIGURE 6

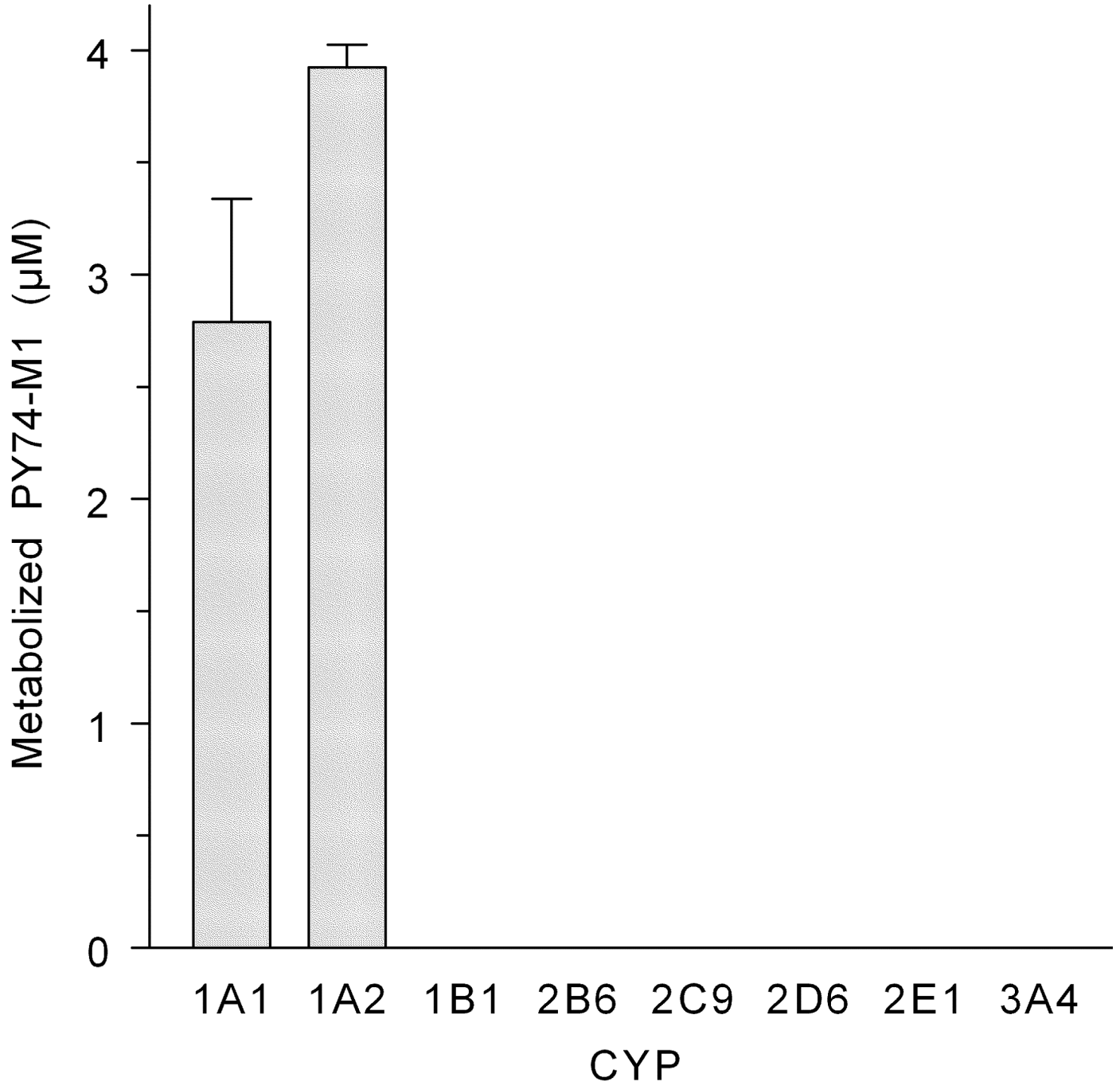

FIGURE 7